Lipid domain formation and ligand–receptor distribution in lipid bilayer membranes investigated by atomic force microscopy

Thomas Kaasgaard[a], Ole G. Mouritsen[b], Kent Jørgensen[a,*]

[a] *Department of Chemistry, Technical University of Denmark, DK-2800 Lyngby, Denmark*
[b] *MEMPHYS-Center for Biomembrane Physics, University of Southern Denmark, Campusvej 55, DK-5230 Odense M, Denmark*

Received 18 December 2001; revised 1 February 2002; accepted 1 February 2002

First published online 22 February 2002

Edited by Felix Wieland

Abstract A novel experimental technique, based on atomic force microscopy (AFM), is proposed to visualize the lateral organization of membrane systems in the nanometer range. The technique involves the use of a ligand–receptor pair, biotin–avidin, which introduces a height variation on a solid-supported lipid bilayer membrane. This leads to a height amplification of the lateral membrane organization that is large enough to be clearly imaged by scanning AFM. The power of the technique is demonstrated for a binary dipalmitoylphosphocholine–diarachidoylphosphocholine lipid mixture which is shown to exhibit a distinct lateral lipid domain formation. The new and simple ligand–receptor-based AFM approach opens up new ways to investigate lipid membrane microstructure in the nanometer range as well as the lateral distribution of ligand–lipid and receptor–protein complexes in supported membrane systems. **© 2002 Federation of European Biochemical Societies. Published by Elsevier Science B.V. All rights reserved.**

Key words: Lipid bilayer membrane; Atomic force microscopy; Lipid membrane heterogeneity; Lipid domain; Langmuir–Blodgett film; Phosphatidylcholine; Lipid mixture; Biotin; Avidin

1. Introduction

The lipid bilayer part of biomembranes is a highly complex two-dimensional structure composed of a variety of different lipids [1,2]. It has become evident in recent years that the lateral organization of the lipid bilayer is far from random or homogeneous, but rather structured in terms of lipid domains [3]. The range of length scales over which these domains persist varies from nanometers up to the size of the whole cell [4–6]. Results from both experimental and theoretical membrane studies have clearly demonstrated that the formation of lipid domains and small-scale lipid structures, in certain contexts called rafts, play an important role as regulating units for a large number of biological functions that take place in or are associated with lipid membranes [3,4,7,8]. Large-scale lipid structures can be stabilized by static thermodynamic phase separation, by coupling via integral membrane proteins to the cytoskeleton, or by locally curved membrane regions [9–11]. Small-scale lipid domain formation is likely to be controlled by the nature of the lipid–lipid interactions [12]. It has been shown that lipid membrane heterogeneity and the formation of micro-domains are of importance for the activity of membrane-associated enzymes and proteins. Specific examples of the close interplay between lipid membrane microstructure and function include the binding and activation of peripheral enzymes and proteins such as phospholipase A_2, cytochrome *c*, and kinase C [13–15].

In recent years, substantial progress has been made in visualizing lipid domains in model membrane systems, in particular large unilamellar liposomes, using various fluorescence microscopy techniques [16–20]. Since the spatial resolution of these techniques is limited by the wavelength of light, the length scale of the detected domain patterns is in the range of micrometers. Modern scanning atomic force microscopy (AFM) techniques lend themselves to extend the spatial scale down towards the nanometer range, provided that the membranes can be fixed on solid supports and provided that the lateral structure is reflected in height variations that can be detected by the tip of the AFM [21]. In this context it should be noted that lipid membranes are soft and may yield to the force exerted by the tip leading to a distorted image. The need therefore arises for a simple, robust, and versatile technique that can be used to directly image by AFM the lateral structure of lipid membranes by a suitable 'amplification' method.

In the present paper, a simple type of ligand–receptor-based binding assay designed to directly visualize lipid domain formation in solid-supported lipid bilayer membranes using AFM is proposed. The method includes headgroup-labeled ligand lipid analogs (biotin-$DC_{16}PE$), which are chosen such that they display a high affinity for putative lipid domains that are expected to be formed in a two-component lipid bilayer membrane composed of $DC_{16}PC$ and $DC_{20}PC$ lipids. The main idea is that if lipid domains are formed resulting in a heterogeneous lateral membrane structure composed of coexisting small-scale lipid structures, the biotin-$DC_{16}PE$ lipids will demix and segregate into those $DC_{16}PC$-rich lipid structures where they have the highest affinity as schematically shown in Fig. 1. Addition of avidin proteins, which bind tightly to the headgroup-labeled biotin lipids [22] will then lead to a preferential binding of avidin proteins to those lipid membrane regions with the highest local density of biotin-$DC_{16}PE$ lipids, e.g. possible phase-separated lipid structures enriched in $DC_{16}PC$ lipids. A related approach using fluorescent lipid analog probes that segregate and accumulate in coexisting gel and fluid phases has previously been used to provide indirect evidence of small-scale lipid structures in various phospholipid vesicular systems [23,24]. By means of in

*Corresponding author. Fax: (45)-45883136.
E-mail address: jorgense@kemi.dtu.dk (K. Jørgensen).

Abbreviations: DC_nPC, saturated di-acyl phosphatidylcholine with *n* carbon atoms in each acyl chain; AFM, atomic force microscopy

0014-5793/02/$22.00 © 2002 Federation of European Biochemical Societies. Published by Elsevier Science B.V. All rights reserved.
PII: S0014-5793(02)02391-8

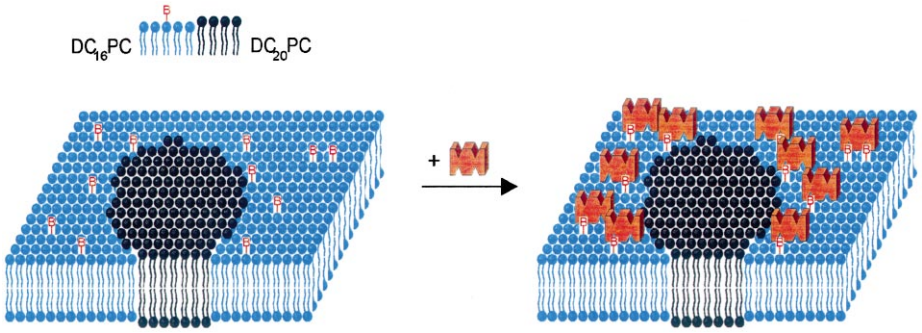

Fig. 1. Schematic illustration of the principle behind the ligand–receptor-based amplification technique designed to detect lipid domains and the lateral distribution of ligand lipids and receptor proteins in lipid bilayer membranes by means of AFM. Left: Phase separation and lipid domain formation in a $DC_{16}PC$–$DC_{20}PC$ mixture containing a small amount of biotin-$DC_{16}PE$ ligand lipids. The biotin-$DC_{16}PE$ lipids are assumed to partition into $DC_{16}PC$-enriched phase structures of the lipid mixture due to favorable lipid–lipid interactions. Right: The added avidin proteins bind to the biotin lipids and thereby accentuate the lipid domains by introducing a large height difference that becomes detectable by AFM.

situ AFM imaging of the surface topography of the lateral membrane structure, a distinct height amplification of small-scale $DC_{16}PC$-rich lipid structures having the 66 kDa avidin proteins tightly bound to the membrane surface will consequently become detectable and show up on the height image. The potential of the method is demonstrated for the two-component $DC_{16}PC$–$DC_{20}PC$ lipid mixture displaying gel–gel phase coexistence as well as for a lipid membrane system with locally curved regions surrounding preexisting holes in a supported lipid bilayer membrane. We have chosen to use a $DC_{16}PC$–$DC_{20}PC$ lipid mixture as an interesting and suitable model system to work with at room temperature in order to learn about the usefulness of the novel AFM technique on the one hand and the lateral membrane organization of a binary lipid mixture on the other hand. The method can easily be extended and used to explore, amplify, and detect small-scale lipid structures in more complex lipid systems, e.g. multi-component lipid bilayer membranes, by choosing suitably designed headgroup-labeled ligand lipid probes with a high affinity to the different types of lipid domains or rafts that are expected to be present in the heterogeneous lipid membrane structure [3,4,7].

2. Materials and methods

The solid-supported lipid bilayers were prepared using Langmuir–Blodgett techniques. The phospholipids $DC_{16}PC$ (1,2-dihexadecanoic-*sn*-glycero-3-phosphocholine) and $DC_{20}PC$ (1,2-dieicosanoic-*sn*-glycero-3-phosphocholine) were obtained from Avanti Polar Lipids. Biotin-$DC_{16}PE$ (biotin-X-1,2-dihexadecanoic-*sn*-glycero-3-phosphoethanolamine) and avidin (avidin-BODIPY-Fl) were from Molecular Probes. Phospholipid monolayers containing a low amount of biotin-$DC_{16}PE$ lipids (0.7 mol%) were formed on a pure milliQ-H_2O subphase using a Langmuir trough (Kibron, Helsinki, Finland) by spreading a 0.5 mg/ml phospholipid solution in hexane:methanol (99:1 v/v). Solvent evaporation was allowed for 30 min prior to monolayer compression at a rate of 2 Å^2/molecule/min to a final lateral pressure of 40 mN/m. Two vertical depositions of the monolayers on freshly cleaved mica were made at a transfer rate of 1 mm/min, leading to a supported bilayer in water. Between the first and the second deposition the monolayer film on the mica plate was allowed to dry in air for 15 min. The subphase temperature was 15°C and the lateral pressure was kept constant at 40 mN/m during the two monolayer depositions as shown by the arrow in Fig. 2. The solid-supported phospholipid bilayers fully immersed in the subphase were transferred to the AFM microscope (PicoSPM, Molecular Imaging, Phoenix, AZ, USA) without exposure to air. The contact-mode AFM images were obtained at room temperature using oxide-sharpened silicon nitride cantilevers (ThermoMicroscopes, Sunnyvale, CA, USA) with nominal spring constants of 0.02 N/m. Images were recorded both before and after addition of avidin. Avidin was added to the aqueous milliQ-H_2O phase to give a total concentration of approximately 100 nM. The lipid concentration of the solid-supported lipid bilayer system was approximately 2 μM.

3. Results and discussion

The compression isotherm for the equimolar $DC_{16}PC$–$DC_{20}PC$ mixture shown in Fig. 2 reflects the macroscopic phase behavior of the lipid monolayer. At a lateral pressure around 15 mN/m, a transition of the monolayer from the liquid-expanded to the liquid-condensed structure takes place. The two monolayer depositions were performed at a lateral pressure of 40 mN/m, where the lipid acyl chains adopt a highly ordered conformation and comprise a monolayer phase structure that resembles the low-temperature conformationally ordered gel phase of lipid bilayer vesicles. Phase diagrams for similar vesicular systems suggest that lipid mixtures composed of phospholipids differing by four methylene units either display or are very close to displaying gel–gel phase coexistence in the low-temperature ordered phase [25,26].

The AFM pictures in Fig. 3 visualize a mica-supported equimolar $DC_{16}PC$–$DC_{20}PC$ lipid bilayer mixture using the ligand–receptor-based amplification approach. The left-hand

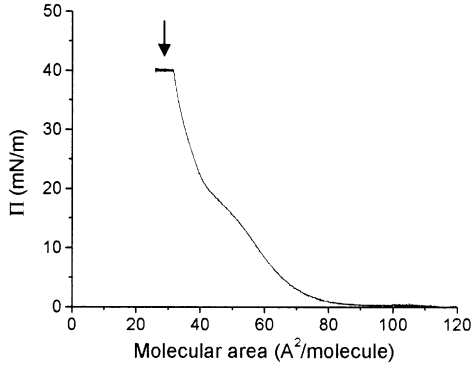

Fig. 2. Compression isotherm for a 1:1 $DC_{16}PC$–$DC_{20}PC$ mixture containing 0.7 mol% biotin-labeled $DC_{16}PE$ lipids. The subphase was pure milliQ-H_2O and the compression rate was 2 Å^2/molecule/min. The monolayer depositions were performed at a constant pressure of 40 mN/m as marked by the arrow.

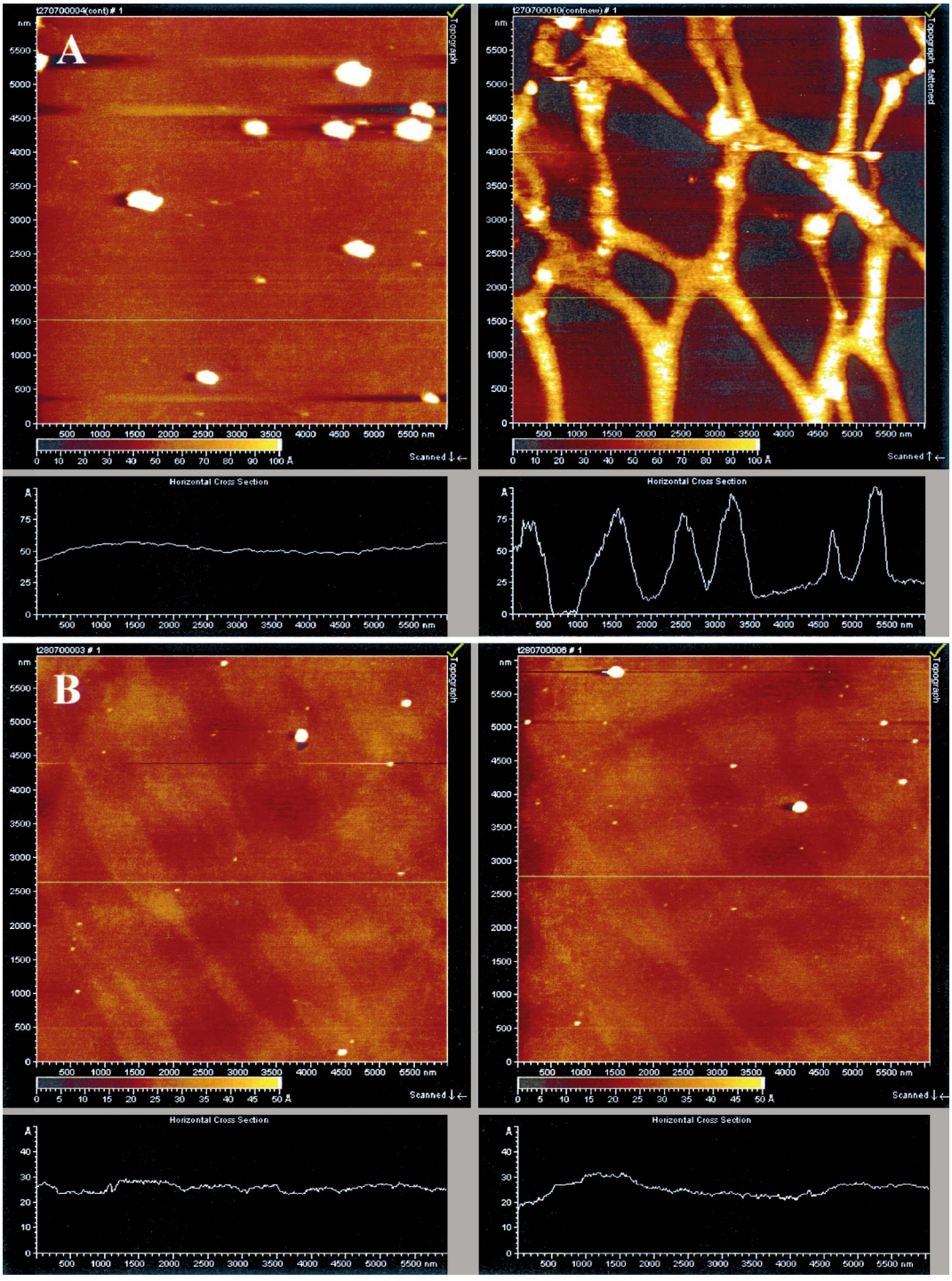

Fig. 3. A: Ligand–receptor-based amplification of lipid domains in an equimolar $DC_{16}PC$–$DC_{20}PC$ mixture. The left-hand image shows a $DC_{16}PC$–$DC_{20}PC$ lipid bilayer containing 0.7 mol% biotin–$DC_{16}PE$ lipids before the addition of avidin proteins. The right-hand image shows the same lipid bilayer membrane after avidin proteins were added. It is observed that the avidin proteins bind to the lipid membrane surface in a distinct pattern due to partitioning of biotin–$DC_{16}PE$ lipids into $DC_{16}PC$-enriched small-scale lipid structures. The size of the images is 6×6 μm^2. B: Control experiment. The left-hand AFM image shows a $DC_{16}PC$–$DC_{20}PC$ lipid mixture having the same composition as the one in A except that no biotin–$DC_{16}PE$ lipid ligands were incorporated. The right-hand image shows the 1:1 $DC_{16}PC$–$DC_{20}PC$ lipid mixture after avidin proteins were added. In contrast to the results shown in A, the addition of avidin proteins does not bring about drastic changes in the surface topography of the $DC_{16}PC$–$DC_{20}PC$ lipid mixture. The size of the images is 6×6 μm^2. It should be noted that the height scale in A is larger than the scale used in B.

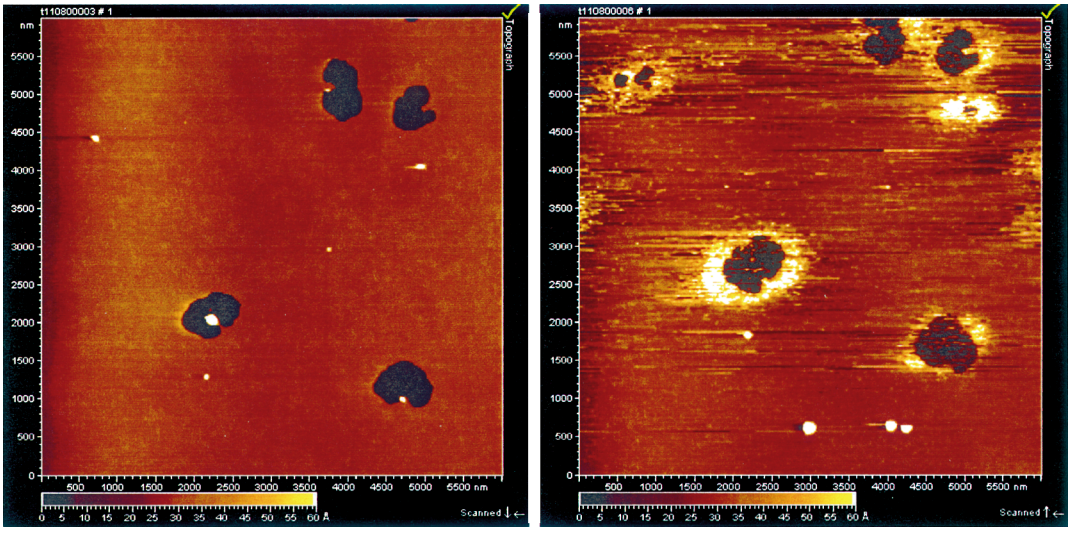

Fig. 4. A lipid bilayer membrane composed of 3:1 $DC_{16}PC$–$DC_{20}PC$ with 0.7 mol% biotin–$DC_{16}PE$ lipids incorporated. The left-hand AFM image shows the lipid membrane before addition of avidin proteins. The black regions are holes in the lipid bilayer membrane. The AFM image shown to the right reveals that the biotin-binding avidin proteins preferentially bind and become located near the pre-formed holes in the lipid bilayer membrane. The size of the images is 6×6 μm^2.

image in Fig. 3A shows a $DC_{16}PC$–$DC_{20}PC$ lipid bilayer containing 0.7 mol% biotin–$DC_{16}PE$ lipids before addition of avidin proteins. Strikingly, the AFM picture reveals a more or less flat membrane surface where the small height differences between putative lipid domains composed mainly of $DC_{16}PC$ or $DC_{20}PC$ lipids are poorly resolved. It should be remarked that the incorporation of 0.7 mol% biotin–$DC_{16}PE$ into $DC_{16}PC$ membranes has an insignificant effect on the phase structure as determined from differential scanning calorimetry data of the main transition (data not shown). The appearance of an almost flat lateral structure of the lipid mixture is further corroborated by the horizontal height profile of the lipid membrane surface shown at the bottom of Fig. 3A. In contrast, on the right-hand AFM height image in Fig. 3A, which shows the same lipid membrane mixture after addition of avidin proteins, a profound heterogeneous lateral membrane structure shows up. Assuming that the biotin–$DC_{16}PE$ lipids partition and accumulate in lipid membrane regions that are enriched in $DC_{16}PC$ lipids, the patterns seen on this AFM image suggest the presence of an underlying heterogeneous lipid membrane structure that is drastically amplified in the AFM scan after addition of the biotin-binding avidin proteins. The measured height differences of around 60–70 Å, shown by the height profile at the bottom of the AFM image in Fig. 3A, reflect that the large 66 kDa avidin proteins are tightly bound to those biotin lipids that have segregated into $DC_{16}PC$-rich lipid domains. In this manner, the height differences can be discerned by AFM. The observed height differences might appear a little high in comparison to earlier AFM studies [27,28] which yielded height differences of 38 Å and 46.5 Å for the structurally similar streptavidin protein. However, in contrast to streptavidin, avidin is positively charged at neutral pH and this charge may result in an additional electrostatic height contribution if some avidin proteins are adsorbed to the negatively charged AFM tip [29]. The detected height differences might also be related to the fact that the streptavidin proteins in the work by Reviakine et al. [27] are in a more compact 2-D crystal-like structure. In addition, the larger size of avidin as well as the fact that Scheuring et al. [28] use a fluid-phase DOPC might also play a role. As a control, the left-hand image in Fig. 3B shows a lipid bilayer having the same composition as the one in Fig. 3A, except that no biotin lipids were incorporated. It should be noted that the height scale in Fig. 3A is larger than the scale used in Fig. 3B. In contrast to the results shown in Fig. 3A, the presence of avidin, as shown on the right-hand image in Fig. 3B, does not bring about drastic changes in the topography of the lipid membrane surface since no ligand biotin lipids required for binding of avidin proteins are present on the lipid membrane surface. This observation strongly suggests that the AFM picture in Fig. 3A is indeed related to the lateral organization of the lipid mixture and that the avidin proteins bind to biotin–$DC_{16}PE$ lipids which are accumulated in the phase-separated lipid domains enriched in $DC_{16}PC$ lipids. Interestingly, lipid domain patterns of similar sizes have been observed by confocal fluorescence microscopy of giant unilamellar vesicles in phosphocholine lipid mixtures [16].

The AFM images in Fig. 4 show a 3:1 $DC_{16}PC$–$DC_{20}PC$ lipid bilayer membrane, with 0.7 mol% biotin–$DC_{16}PE$ incorporated, before and after addition of avidin. After deposition of the two lipid monolayers on the solid mica support, some minor holes in the lipid bilayer membranes were observed on the AFM images (cf. Figs. 3 and 4) [30]. The depth of the holes shown as black regions on the images in Fig. 4 is around 75 Å, corresponding to a mica-supported $DC_{16}PC$ lipid bilayer in the ordered state [30]. From the right-hand AFM picture in Fig. 4 it is observed that addition of avidin proteins induces a height difference in those membrane regions that surround the preexisting holes. This observation suggests that the avidin proteins in the 3:1 $DC_{16}PC$–$DC_{20}PC$ mixture bind to biotin–$DC_{16}PE$ lipids that predominantly are located in the vicinity of the holes. It is conceivable that these highly curved and disordered boundary regions [31] favor a preferential distribution and accumulation of the bulky headgroup-labeled biotin–$DC_{16}PE$ lipids and the $DC_{16}PC$ lipids, whereas the acyl chain matching is expected to play a minor role.

Consequently, the biotin-binding avidin proteins become located in the same partly disordered and curved membrane regions as suggested by the AFM image in Fig. 4.

We have in this work proposed a novel, simple, and powerful ligand–receptor-based AFM method to investigate small-scale structures in lipid bilayer membranes. We have presented in situ AFM results which demonstrate that this approach can be used to detect different macroscopic lipid phases and small-scale lipid structures in lipid bilayer membranes. The surface scanning AFM approach provides evidence of a preferential binding of proteins to lipid domains that are likely to persist on various length scales in the heterogeneous lipid membrane. We have used the novel method to obtain direct experimental evidence for lipid domain formation in a simple and well-defined $DC_{16}PC$–$DC_{20}PC$ lipid membrane mixture in the gel–gel phase coexistence region. The obtained results suggest that it is possible and straightforward to refine and extend this type of simple design, e.g. by using lipid ligand probes that are specifically designed to have high affinity for certain types of lipid domains and lipid membrane micro-environments. It can be argued that height amplification of lipid domains is unnecessary since height differences corresponding to a four carbon atom disparity in chain length have been previously visualized by AFM [32]. That study, like the present study, was performed using mica as the solid support. Mica gives high resolution AFM images because it is solid and therefore does not yield to the force of the AFM tip and because it is atomically flat over large length scales. There are, however, indications that the mica support may influence bilayer behavior [33,34] and it is therefore reasonable to believe that other supported membrane systems will find use in future studies. Polymer-cushioned membranes [35] and supported double membranes [33] are likely candidates for such unperturbed model membrane systems. The improved resemblance to free-standing membrane behavior that these systems are likely to display may be at the cost of lateral as well as vertical resolution in the AFM images and height amplification of domains might therefore become essential in these systems. Furthermore, it can become necessary to amplify height differences in mica-supported membranes if the desired scan area is large since the resolution in the z-direction decreases when the scan area is increased because of the intrinsic non-linearity of piezo-scanners. Also, if an additional non-linear contribution exists from using a support which is not completely flat or is very soft, it becomes more complicated to perform an appropriate background correction and a proper height amplification method may consequently become necessary.

The size and time scales of lipid domain formation in lipid bilayer membranes is expected to be strongly influenced by the composition of the system. In principle, lipid domains can be from a few nanometers to macroscopic sizes and characterized by a lifetime that can vary from milliseconds to hours [4,36,37]. The AFM height imaging approach reported in the present paper can readily be extended to study lipid domain formation and small-scale lipid structures in more complex lipid mixtures where compositional fluctuations may prevail [38] and lead to the formation of equilibrium and non-equilibrium small-scale lipid structures of different geometries, sizes, and lifetimes [4]. In particular, the non-equilibrium formation of coexisting lipid domains characterized by a relaxation time on the order of hours can easily be monitored [37].

The novel and simple ligand–receptor-based AFM approach opens up new ways to investigate the formation and presence of lipid domains and rafts in complex lipid membrane mixtures [3,7,39,40] by using specific ligand lipids, e.g. biotin-labeled cholesterol or sphingomyelin derivatives which can be designed to accumulate in certain small-scale membrane structures.

Acknowledgements: This work was supported by the Apoteker Foundation of 1991, the Hasselblad Foundation, and the Danish Medical Research Council via a grant to the Centre for Drug Design and Transport. MEMPHYS-Center for Biomembrane Physics is supported by the Danish National Research Foundation.

References

[1] Gennis, R.B. (1989) Biomembranes. Molecular Structure and Function, Springer-Verlag, London.
[2] Baszkin, A. and Norde, W. (2000) Physical Chemistry of Biological Interfaces, Marcel Dekker, New York.
[3] Bergelson, L.O., Gawrisch, K., Ferretti, J.A. and Blumenthal, R. (1995) Mol. Membr. Biol. 12, 1–162.
[4] Mouritsen, O.G. and Jørgensen, K. (1997) Curr. Opin. Struct. Biol. 7, 518–527.
[5] Glaser, M., Wanaski, S., Buser, C.A., Boguslavsky, V., Rashidzada, W., Morris, A., Rebecchi, M., Scarlata, S.F., Runnels, L.W., Prestwich, G.D., Chen, J., Aderem, A., Ahn, J. and McLaughlin, S. (1996) J. Biol. Chem. 271, 26187–26193.
[6] Edidin, M. (1997) Curr. Opin. Struct. Biol. 7, 528–532.
[7] Brown, D.A. and London, E. (1998) Annu. Rev. Cell Dev. Biol. 14, 111–136.
[8] Simons, K. and Ikonen, E. (1997) Nature 387, 569–572.
[9] Kusumi, A. and Yashushi, S. (1996) Curr. Opin. Cell Biol. 8, 566–574.
[10] Sackmann, E. (1994) FEBS Lett. 346, 3–16.
[11] Trandum, C., Westh, P. and Jørgensen, K. (1999) Biochim. Biophys. Acta 1421, 207–212.
[12] Nielsen, L.K., Vishnyakov, A., Jørgensen, K., Bjørnholm, T. and Mouritsen, O.G. (2000) J. Phys. Condens. Matter 12, 309–314.
[13] Hønger, T., Jørgensen, K., Biltonen, R.L. and Mouritsen, O.G. (1996) Biochemistry 35, 9003–9006.
[14] Kinnunen, P.K.J. (1996) Chem. Phys. Lipids 81, 151–166.
[15] Yang, L. and Glaser, M. (1996) Biochemistry 35, 13966–13974.
[16] Korlach, J., Schwille, P., Webb, W.W. and Feigenson, G.W. (1999) Proc. Natl. Acad. Sci. USA 96, 8461–8466.
[17] Bagatolli, L.A. and Gratton, E. (1999) Biophys. J. 77, 2090–2101.
[18] Bagatolli, L.A. and Gratton, E. (2000) Biophys. J. 79, 434–447.
[19] Dietrich, C., Bagatolli, L.A., Volovyk, Z.N., Thomson, N.L., Levi, M., Jacobsen, K. and Gratton, E. (2001) Biophys. J. 80, 1417–1428.
[20] Feigenson, G.W. and Bubolz, J.T. (2001) Biophys. J. 80, 2775–2788.
[21] Tamm, L.K. and Shao, Z. (1998) in: Biomembrane Structure (Chapman, D. and Haris, P., Eds.), pp. 169–185, IOS Press, Amsterdam.
[22] Kaasgaard, T., Mouritsen, O.G. and Jørgensen, K. (2001) J. Liposome Res. 103, 31–42.
[23] Pedersen, S., Jørgensen, K., Bækmark, T. and Mouritsen, O.G. (1996) Biophys. J. 71, 554–560.
[24] Leidy, C., Wolkers, W.F., Jørgensen, K., Mouritsen, O.G. and Crowe, J.H. (2001) Biophys. J. 80, 1819–1828.
[25] Knoll, W., Schmidt, G., Rötzer, H., Henkel, T., Pfeiffer, W., Sackmann, E., Mittler-Neher, S. and Spinke, J. (1991) Chem. Phys. Lipids 57, 363–374.
[26] Schram, V., Lin, H.N. and Thompson, T.E. (1996) Biophys. J. 71, 1811–1822.
[27] Reviakine, I. and Brisson, A. (2001) Langmuir 17, 8293–8299.
[28] Scheuring, S., Müller, D.J., Ringler, P., Heymann, J.B. and Engel, A. (1999) J. Microsc. 193, 28–35.
[29] Müller, D.J. and Engel, A. (1997) Biophys. J. 73, 1633–1644.
[30] Rinia, H.A., Demel, R.A., van der Eerden, J.P.J.M. and de Kruijff, B. (1999) Biophys. J. 77, 1683–1693.
[31] Grandbois, M., Clausen-Schaumann, H. and Gaub, H. (1998) Biophys. J. 74, 2398–2404.

[32] Gliss, C., Clausen-Schaumann, H., Gunther, R., Odenbach, S., Randl, O. and Bayerl, T.M. (1998) Biophys. J. 74, 2443–2450.
[33] Fragneto, G., Charitat, T., Graner, F., Mecke, K., Perino-Gallice, L. and Bellet-Amalric, E. (2001) Europhys. Lett. 53, 100–106.
[34] Yang, J. and Appleyard, J. (2000) J. Phys. Chem. B 104, 8097–8100.
[35] Wong, J.Y., Majewski, J., Seitz, M., Park, C.K., Israelachvili, J.N. and Smith, G.S. (1999) Biophys. J. 77, 1445–1457.
[36] van Osdol, W.W., Johnson, M.L., Ye, Q. and Biltonen, R.L. (1991) Biophys. J. 59, 775–785.
[37] Jørgensen, K., Klinger, A. and Biltonen, R.L. (2000) J. Phys. Chem. B 104, 11763–11773.
[38] Jørgensen, K., Sperotto, M.M., Mouritsen, O.G., Ipsen, J.H. and Zuckermann, M.J. (1993) Biochim. Biophys. Acta 1152, 135–145.
[39] Brown, D.A. and London, E.J. (1998) Membr. Biol. 164, 475–481.
[40] Rinia, H.A., Snel, M.M.E., van der Eerden, J.P.J.M. and de Kruijff, B. (2001) FEBS Lett. 501, 92–96.